Usage Report for Fiscal Year 2024

Project Title:

A Computational Investigation of Intermolecular Interactions in Room Temperature Ionic Liquid by Using μ as a Probe.

Name:

○Michael Armstrong (1), Jaikaew Phantip (1), Charoenphon Supparat (1), Zaharim Binti Wan Nurfadhilah (1), Ramadhan Redo Muhammad (1), Puspita Sari Dita (1), Ramli Irwan (1)

Laboratory at RIKEN:

(1) RIKEN Nishina Center for Accelerator-Based Science, Meson Science Laboratory

---

1. Background and purpose of the project

In the past decade, room-temperature ionic liquid (RTIL) has gained attention due to its wide functionality. Although a concrete of its usefulness in RTIL is established, we have limited understanding in the microscopic behavior of how RTIL interacts with each other. Moreover, since RTIL is a combination of molecular cation and anion, polymorphic behavior occurs instead of an even dissipation of such ions as an ion-pair structure.[1] Thus, both computational and experimental studies were conducted to decipher such behavior where each RTIL combination showed a distinct morphological characteristic which lead to the unique bulk properties in each variation.[2]

To further extend the understanding of behavioral characteristics of RTIL, muon spectroscopy (μSR) can be a promising non-invasive approach to observing the morphology in RTIL. Despite the limited use of μSR at the current state, we speculated that the use of μ to probe the characteristic can give us the local interaction of RTIL without adding molecular probe which would disrupt the bulk structure.

Therefore, the computational study of four well-known RTIL combinations was conducted to find a possibility of implanting μ particle for the future μSR experiments. A combination of classical molecular dynamics simulations and first-principal calculations were implemented in this study to refine the accuracy of its physical properties before conducting a further μ implantation.

2. Specific usage status of the system and calculation method

2.1 Molecular Structure of the studied RTILs

To systematically compare the structural characteristics of our interested RTIL (figure 1), we varied the molecular anion including *bis*(trifluoromethyl sulfonil)imide ($[NTf_2]^-$), tetrafluoroborate ($[BF_4]^-$), hexafluorophosphate ($[PF_6]^-$), and chloride ion ($[Cl]^-$) while the molecular cation used with those anion is 1-ethyl-3-methylimidazolium cation ($[C_2mim]^+$).

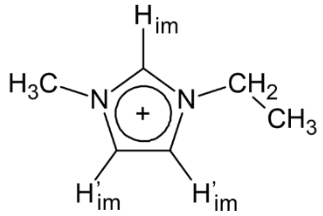

1-ethyl-3-methylimidazolium ($[C_2mim]^+$)

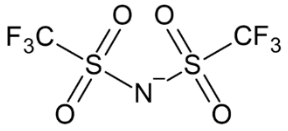

bis(trifluoromethyl sulfonyl)imide ($[NTf_2]^-$)

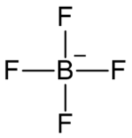

tetrafluoroborate ($[BF_4]^-$)

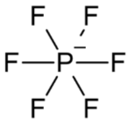

hexafluorophosphate ($[PF_6]^-$)

Cl^-

chloride ($[Cl]^-$)

Figure 1. Molecular structures of the studied RTIL, comparing 4 different anions pairing with same cation. The H atoms in imidazolium ring of $[C_2mim]^+$ were coded as H_{im} and H'_{im}.

2. 2 Classical molecular dynamic simulation

Initially classical molecular dynamic simulations were conducted by using LAMMPS package version 29 Aug 2024.[3] Cl&Pol forcefield was implemented for all RTIL in this study.[4, 5] Each simulation box was filled with 800 ion pairs of each RTIL combination ([C_2mim][NTf_2], [C_2mim][BF_4], [C_2mim][PF_6], and [C_2mim][Cl]). The simulation started with initial heating from 0 K to 298 K within 0.5 ns, followed by simulated annealing where we rapidly increased the temperature of the box up to its thermal stability threshold at letting it gradually relaxed back to 298 K. Due to the high viscosity of the RTILs, we need to perform such step to accelerate the simulation time and to reach the most stable molecular assembly state. Next, each box was kept simulating at a constant temperature of 298 K for 10.0 ns to ensure the equilibrium state. The procedure above were run under isothermal–isobaric (NPT) ensemble with a constant pressure of 1.0 atm. Finally, a production run was performed to collect the dynamical properties of each box within 10.0 ns. The production run was performed under the canonical (NVT) ensemble at a constant temperature of 298 K. The temperature and pressure in the simulation was regulated by Nosé-Hoover thermostat.[6, 7] The timestep of trajectory calculations was 1.0 fs. We collected every output including initial results and trajectories at every 1000 fs.

Since [C_2mim][PF_6] and [C_2mim][Cl] are solid at 298 K,[8, 9] we constructed another simulation box for each variation and repeated the procedure, but increased the temperature to 353 K.

2. 3 Density functional theory (DFT) calculations

The trajectory files of each variation during production run were exported to obtain the coordination of each particle in the box. The whole structure in the box was averaged within the last 0.2 ns (total of 200 frames) before 4 ion pairs structures in the center of the simulation box were extracted. Each extracted ion pair was carried on to density functional theory (DFT) calculation by using Gaussian software version 16_C.02.[10] Input file generation and visualization were conducted by GaussView visualizer version 6.0.16.[11] Each software was provided by Hokusai Big Waterfall 2 supercomputer.

An initial structure for each variation at 298 K was depicted as shown in figure 2. A geometry optimization of each structure was conducted followed by IR frequency calculation and electrostatic potential map calculations by using B3LYP with Grimme's dispersion correction (D3) where cc-pvtz basis set were implemented.[12-15] Intermolecular interactions visualizations were produced by BIOVIA Discovery Studio Visualizer version 25.1.0.024284.[16]

This study utilized 24.8% of the total CPU core hour in MPC, HBW2. A total storage of 553 GB was used in this project.

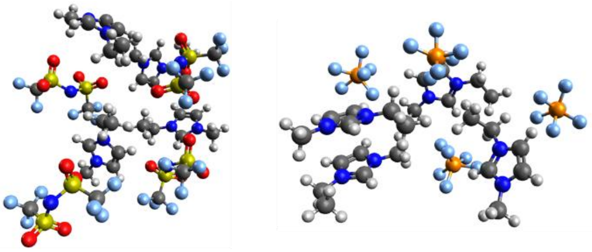

[C_2mim][NTf_2] [C_2mim][PF_6]

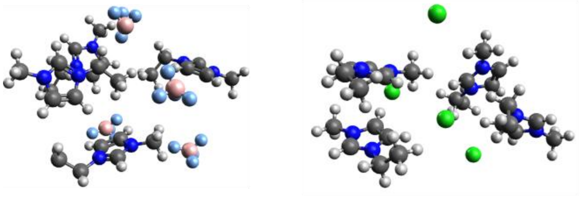

[C_2mim][BF_4] [C_2mim][Cl]

Figure 2. Initial the 4 ion pairs structures of [C_2mim][NTf_2], [C_2mim][BF_4], [C_2mim][PF_6], and [C_2mim][Cl]. Each structure was extracted from the molecular dynamic simulation

3． Result

3. 1 Classical molecular dynamic simulation results

The molecular dynamic simulations of each RTIL at 298 K (figure 3a) showed a slight property deviation in terms of density in [C_2mim][NTf_2], [C_2mim][BF_4] and [C_2mim][PF_6]. However, density of [C_2mim][Cl] possessed 22.5%

deviation which may due to the inappropriate parameterization in solid state. The suspected error was further proved at 353 K (figure 3b) where the deviation reduced to 10.0%. Interestingly, the density of RTILs decreased from the largest anion $[NTf_2]^-$ to the smallest $[Cl]^-$. In addition, the trend of density may relate to the number of interaction sites in anion which plays a crucial role in molecular assembly in RTIL.[17]

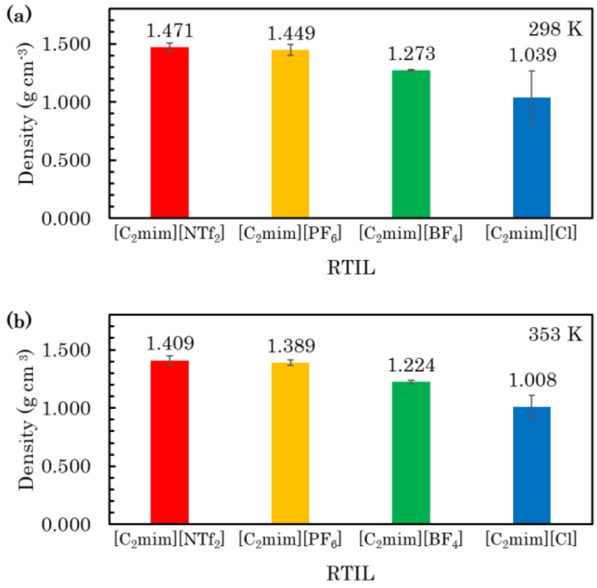

Figure 3. Density of each RTIL at (a) 298 K and (b) 353 averaged at the last 0.5 ns during production run.

To further investigate the local interaction of each RTIL, a coordination number (C.N.) was calculated by an accumulative integration of radial distribution function for any neighboring structure between H in $[C_2mim]^+$ and highly electronegative (EN) atoms in each anion as shown in figure 4. The C.N. corresponds to the number of surrounding atoms respected to H atom within the observing radius. At 298 K (Figure 4a), the surrounding highly EN species respected to H in CH_3 below 4.0 Å were noticeably lower than other sites in $[C_2mim][PF_6]$, $[C_2mim][BF_4]$ and $[C_2mim][Cl]$ while C.N. of each H site in $[C_2mim][NTf_2]$ slightly differed. As mentioned that $[C_2mim][PF_6]$ and $[C_2mim][Cl]$ are solid at 298 K, we observed a drastic shift of C.N. at 353 K where a H sites shared relatively the same amount of surrounding atoms which reasonable for conventional liquid. Interestingly, the C.N. between H_{CH3} and F atoms in $[C_2mim][BF_4]$ shared a similar structure to $[C_2mim][PF_6]$ even though $[C_2mim][BF_4]$ is in liquid state at both temperatures. Furthermore, the $[Cl]^-$ ion moved away from the cation ion at 353 K, indicating that the movement of the chloride anion was less restricted.

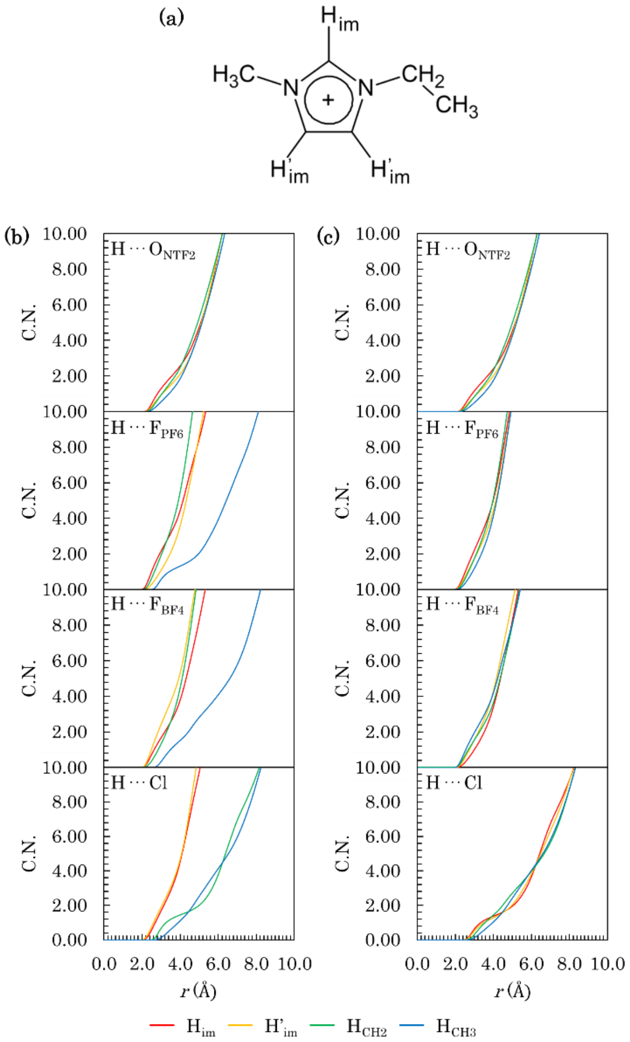

Figure 4. (a) A molecular structure of $[C_2mim]^+$ and coordination numbers (C.N.) highly electronegative atoms at (b) 298 K and (c) 353 K in each anion respected to each H atom site in $[C_2mim]^+$.

3. 2 DFT calculation results at 298 K

Up to the day that this report was produced, DFT calculations of 353 K were still incomplete. Thus, we can only report the results at 298 K. Initially, the optimized structures were visualized to investigate any possible intermolecular interaction as shown in figure 5. As $[NTf_2]^-$ possesses more highly EN atoms than others, accompanied with its high flexibility, the anions can rotate their structure to wrap around the cations where a mixed interaction between conventional H-bond and F-π interaction were abundantly presented. The F-π interaction was a unique interaction only found in $[C_2mim][NTf_2]$ relatively to $[C_2mim][BF_4]$ and $[C_2mim][PF_6]$ in which the interaction is generally known to be a weak interaction, but can be achieved by free rotation in a flexible molecule.[18] In both $[C_2mim][NTf_2]$ and $[C_2mim][PF_6]$, we observed σ-π interactions between lone pair electron in highly EN species and imidazolium ring. In $[C_2mim][BF_4]$, only H-bond was found in the structure which also had the least number of interactions. Prior to the result, very few H-bond interactions and various ionic interactions were expected in $[C_2mim][Cl]$ due to its high melting point. However, the calculation showed that the RTIL has substantial amount of H-bond along with ionic interactions and a π-π interaction between two cations.

Although H-bond interactions were found more than expected, $[C_2mim][Cl]$ is the only RTIL that has ionic interactions which explained why the ionic liquid has a higher melting point than other studied RTIL. Among all intermolecular interactions, ionic attractions are fundamentally known to be one of the strongest interactions in ionic species as cation and anion are attracted by electrostatic differences which are commonly found in common salt such as NaCl, giving its highly stable feature in nature. It is worth noting that other RTILs also possess electrostatic attraction to their counter-ion but may be hindered by the molecular geometry or obstruction from H-bond.[19]

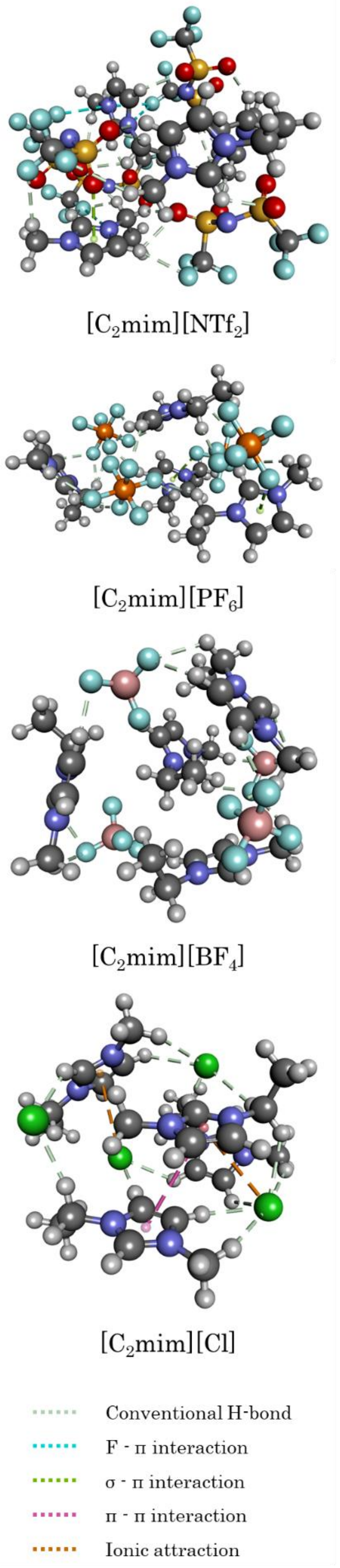
$[C_2mim][NTf_2]$

$[C_2mim][PF_6]$

$[C_2mim][BF_4]$

$[C_2mim][Cl]$

Figure 5. Molecular structure visualization with intermolecular interactions of $[C_2mim][NTf_2]$, $[C_2mim][PF_6]$, $[C_2mim][BF_4]$ and $[C_2mim][Cl]$ where light green dash line is a conventional H-bond, light blue is fluorine-pi (F-π) interaction, olive green is sigma-pi (σ-π) interaction, pink is pi-pi (π-π) interaction and orange is ionic attraction.

4. Conclusion

Computational studies of 4 RTILs including $[C_2mim][NTf_2]$, $[C_2mim][PF_6]$, $[C_2mim][BF_4]$ and $[C_2mim][Cl]$ were conducted to observe the possibility of using μSR for probing its nanostructure. A hybrid simulation started from classical molecular dynamic simulation followed by DFT calculations of the extracted ions. Our molecular dynamic simulation showed a realistic property in $[C_2mim][NTf_2]$, $[C_2mim][PF_6]$ and $[C_2mim][BF_4]$ at both observed temperatures (298 K and 353 K) while $[C_2mim][Cl]$ give a better accuracy at 353 K. The local neighboring structure of $[C_2mim][NTf_2]$ were found to be almost unchanged when varied the temperature. The other three RTILs showed a noticeable shift in local structure especially at the alkyl group in cation. Lastly, we were able to depict several intermolecular interactions in the DFT calculation from the extract ions at 298K. Such information is essential for determining μ implantation site and for observing how μ would perturb the local interaction.

5. Schedule and prospect for the future

The DFT calculation of the extracted ions at 353 K will be carried out along with a further analysis in the calculated electronic structure and electrostatic potential profile of each RTIL. After addressing all necessary electronic and physical properties, muonium (μ^+) will be implanted in the appropriate site where we will determine the effect on μ^+ affecting the local structure as well as the hyperfine coupling interactions in each implantation.

6. References

1. Z. He and P. Alexandridis, *Physical Chemistry Chemical Physics*, 2015, **17**, 18238-18261.
2. W. Zheng, A. Mohammed, L. G. Hines, Jr., D. Xiao, O. J. Martinez, R. A. Bartsch, S. L. Simon, O. Russina, A. Triolo and E. L. Quitevis, *The Journal of Physical Chemistry B*, 2011, **115**, 6572-6584.
3. A. P. Thompson, et al. *Computer Physics Communications*, 2022, **271**, 108171.
4. K. Goloviznina, J. N. Canongia Lopes, M. Costa Gomes and A. A. H. Pádua, *Journal of Chemical Theory and Computation*, 2019, **15**, 5858-5871.
5. K. Goloviznina, Z. Gong, M. F. Costa Gomes and A. A. H. Pádua, *Journal of Chemical Theory and Computation*, 2021, **17**, 1606-1617.
6. W. G. Hoover, *Physical Review A*, 1985, **31**, 1695-1697.
7. S. Nosé, *The Journal of Chemical Physics*, 1984, **81**, 511-519.
8. A. Efimova, L. Pfützner and P. Schmidt, *Thermochimica Acta*, 2015, **604**, 129-136.
9. H. Sakhaeinia, A. H. Jalili, V. Taghikhani and A. A. Safekordi, *Journal of Chemical & Engineering Data*, 2010, **55**, 5839-5845.
10. M. J. Frisch, et al. *Journal*, 2016.
11. T. A. K. a. J. M. M. Roy Dennington, *Journal*, 2019.
12. A. D. Becke, *Physical Review A*, 1988, **38**, 3098-3100.
13. A. D. Becke, *The Journal of Chemical Physics*, 1993, **98**, 5648-5652.
14. C. Lee, W. Yang and R. G. Parr, *Physical Review B*, 1988, **37**, 785-789.
15. T. H. Dunning, Jr., K. A. Peterson and A. K. Wilson, *The Journal of Chemical Physics*, 2001, **114**, 9244-9253.
16. D. S. BIOVIA, *Journal*, 2025.
17. K. Dong, S. Zhang and J. Wang, *Chemical Communications*, 2016, **52**, 6744-6764.
18. F. Philippi, D. Rauber, O. Palumbo, K. Goloviznina, J. McDaniel, D. Pugh, S. Suarez, C. C. Fraenza, A. Padua, C. W. M. Kay and T. Welton, *Chemical Science*, 2022, **13**, 9176-9190.
19. J. G. McDaniel and A. Yethiraj, *The Journal of Physical Chemistry B*, 2019, **123**, 3499-3512.